Acta Pharmacologica Sinica (2014) 35: 697–706

www.nature.com/aps

Original Article

Cordyceps sinensis protects against liver and heart injuries in a rat model of chronic kidney disease: a metabolomic analysis

Xia LIU[2, #], Fang ZHONG[1, #], Xu-long TANG[2, #], Fu-lin LIAN[2], Qiao ZHOU[1], Shan-mai GUO[1], Jia-fu LIU[3], Peng SUN[2], Xu HAO[1], Ying LU[1], Wei-ming WANG[1, *], Nan CHEN[1], Nai-xia ZHANG[2, *]

[1]Department of Nephrology, Ruijin Hospital, School of Medicine, Shanghai Jiao Tong University, Shanghai 200025, China; [2]Department of Analytical Chemistry, Shanghai Institute of Materia Medica, Chinese Academy of Sciences, Shanghai 201203, China; [3]Blood Research Institute, Blood Center of Wisconsin, Milwaukee, WI 53226, USA

Aim: To test the hypothesis that the traditional Chinese medicine *Cordyceps sinensis* could improve the metabolic function of extrarenal organs to achieve its anti-chronic kidney disease (CKD) effects.
Methods: Male SD rats were divided into CKD rats (with 5/6-nephrectomy), CKD rats treated with *Cordyceps sinensis* (4 mg·kg^{-1}·d^{-1}, *po*), and sham-operated rats. After an 8-week treatment, metabolites were extracted from the hearts and livers of the rats, and then subjected to ^{1}H-NMR-based metabolomic analysis.
Results: Oxidative stress, energy metabolism, amino acid and protein metabolism and choline metabolism were considered as links between CKD and extrarenal organ dysfunction. Within the experimental period of 8 weeks, the metabolic disorders in the liver were more pronounced than in the heart, suggesting that CKD-related extrarenal organ dysfunctions occurred sequentially rather than simultaneously. Oral administration of *Cordyceps sinensis* exerted statistically significant rescue effects on the liver and heart by reversely regulating levels of those metabolites that are typically perturbed in CKD.
Conclusion: Oral administration of *Cordyceps sinensis* significantly attenuates the liver and heart injuries in CKD rats. The ^{1}H NMR-based metabolomic approach has provided a systematic view for understanding of CKD and the drug treatment, which can also be used to elucidate the mechanisms of action of other traditional Chinese medicines.

Keywords: *Cordyceps sinensis*; chronic kidney disease; liver injury; heart injury; metabolomics; nuclear magnetic resonance; traditional Chinese medicine

Acta Pharmacologica Sinica (2014) 35: 697–706; doi: 10.1038/aps.2013.186; published online 17 Mar 2014

Introduction

Chronic kidney disease (CKD) is a condition in which the kidney progressively loses its function, and this process can quickly lead to deleterious effects in distant organs. Clinical and experimental data suggest that most forms of CKD contribute to the development and aggravation of distant organ dysfunction, such as heart failure[1, 2] and liver failure[3]. The physiological and molecular mechanisms linking CKD with extrarenal organ dysfunction are complicated. Systematic disturbances of metabolism, which include glomerular hypertension, oxidative stress, progressive azotemia, glycemia, anemia, dyslipidemia *etc*[4], might play important roles in the development of the distant organ dysfunctions related to CKD. However, the molecular mechanism that mediates the cross-talk between kidney disease and extrarenal impairments remains poorly understood.

Because CKD seriously endangers human health, multiple therapeutic agents have been developed to treat the disease. In recent years, in addition to conventional therapies, traditional Chinese medicines (TCMs) began to play important roles in the treatment of CKD. Both clinical evidence and experimental studies have shown the efficacies of TCMs in slowing the progression of CKD[5–8]. Among all the TCMs with anti-CKD effects, *Cordyceps sinensis* (*C sinensis*) is one of the best known. As we reported previously, the renoprotective efficacy of *C sinensis* was confirmed by its ameliorating metabolic abnor-

# These authors contribute equally to this work.
* To whom correspondence should be addressed.
E-mail naixiazhang@mail.shcnc.ac.cn (Nai-xia ZHANG);
wweiming@medmail.com.cn (Wei-ming WANG)
Received 2013-09-18 Accepted 2013-12-06

malities in the kidneys of rats with CKD[9]. Additionally, *C sinensis* has also been identified to play significant roles in the protection of liver[10] and heart[11, 12] tissue from pathological impairments; thus, we hypothesized that *C sinensis* could also improve the metabolic function of the extrarenal organs, such as the heart and liver, to achieve its therapeutic effects on the kidney.

To test this hypothesis and elucidate the possible molecular links mediating the cross-talk between kidney injury and extrarenal impairments, a systematic methodology involving metabolomics was employed. Metabolomics is defined as the comprehensive and quantitative metabolic analysis of large numbers of endogenous, low-molecular-weight metabolites. In the past decade, the widespread utility of this analytical approach to monitoring multiple metabolic perturbations in living systems within pathological processes[13–19], including CKD[17], and the response to such external stimuli as drug treatments[20, 21] has been illustrated. Moreover, this method is now being applied to the field of TCM[22–26], as it could characterize the subtle metabolic interventions induced by TCM in the treatment of diseases and identify the potential implications of TCM. Therefore, in this study, an ^{1}H NMR-based metabolomic study was applied to investigate the extrarenal therapeutic effects of *C sinensis* upon 5/6 nephrectomized (5/6Nx) rats (a standard animal model with CKD[27, 28]). First, a *C sinensis*-dosed 5/6Nx rat group, a 5/6Nx model group and a sham-operated group were established in the study. Then, the changes in the metabolic phenotype of the livers and hearts were investigated using principal component analysis (PCA) and partial least square-discriminant analysis (PLS-DA) of the ^{1}H NMR data. Orthogonal projection to latent structures discriminant analysis (OPLS-DA) was also employed to identify the disturbed metabolites in the model group and the recovery of the metabolic variations in *C sinensis*-dosed 5/6Nx rats. Finally, the potential protective mechanism of *C sinensis* against CKD through its therapeutic effects on extrarenal organs was elucidated based on the analyses mentioned above. In addition, our results also indicated that in the experimental time scale (8 weeks), much more severe liver, but not heart, metabolic disorders occurred. This result suggests that CKD-related extrarenal organ dysfunctions occur sequentially rather than simultaneously.

Materials and methods

Materials

$NaH_2PO_4{\cdot}2H_2O$ and $Na_2HPO_4{\cdot}12H_2O$ (both analytical grade) were provided by merchandisers of Sinopharm Chemical Reagent Co Ltd (Shanghai, China). D_2O (99.9% in D) was purchased from Cambridge Isotope Laboratories Inc (Miami, FL, USA). *C sinensis* was obtained from Jiminkexin Co Ltd (Jiangxi, China). According to the regulation of the Chinese Pharmacopoeia 2005, *C sinensis* was quality controlled by ZGPR-NMR. The contents of two signature components, which were present in the NMR fingerprint profile (Figure S1), were 3.49 mg/g for adenosine and 4.78 mg/g for uridine.

Animal experiments

Animal use protocols, which followed the Guide for the Care and Use of Laboratory Animals, were approved and supervised by the Institutional Animal Care and Use Committee (IACUC) of the Shanghai Institute of Materia Medica, Chinese Academy of Sciences, China. Male Sprague-Dawley rats (130-150 g in weight) were purchased from the Shanghai Experimental Animal Center of the Chinese Academy of Sciences (Shanghai, China). All animals were provided with a certified standard diet and tap water *ad libitum* during the experiments. They were housed at 25±2 °C with 40%–60% humidity and a 12/12-h light/dark cycle. All animals were acclimated for 7 d before experiments.

Experimental animals were randomly divided into three groups: (A) an oral administration of *C sinensis* (4 $mg{\cdot}kg^{-1}{\cdot}d^{-1}$) nephrectomized group (CS group, n=7); (B) an untreated nephrectomized group (OP group, n=7); (C) a sham-operated group (SO group, n=7). The 5/6Nx was performed by a two-step method as described previously[29, 30]. For the SO control group, a sham operation was performed that consisted of a laparotomy and manipulation of the renal pedicles but without the destruction of renal tissue. One animal in the CS group died on the 6th d after the operation and was excluded in the later experiments. On the 8th weekend after surgery, rats from each group were anaesthetized with diethyl ether (Changshu Chemical Co, Ltd, Jiangsu, China), and parts of the livers (approximately 100 mg) and hearts (approximately 100 mg) were collected for ^{1}H NMR spectrum acquisition.

Preparation of aqueous liver and heart extracts and acquisition of ^{1}H NMR spectra

Lyophilized aqueous liver and heart extracts were prepared using the methanol/chloroform/water system as described previously[31]. The powder of the extract was dissolved in 600 μL of phosphate buffer (0.2 mol/L Na_2HPO_4/0.2 mol/L NaH_2PO_4 pH 7.4), vortexed and then centrifuged at 12 000×g for 10 min at 4 °C. Aliquots of the supernatant (500 μL) were transferred into 5-mm diameter NMR tubes, and then 50 μL of D_2O was added. Solvent-suppressed 1D ^{1}H NOESY spectra (NoesyPr1d) were acquired using the pulse sequence (RD-90-t_1-90-t_m-90-ACQ) with a mixing time (t_m) of 100 ms. Water suppression was achieved by irradiation of the water resonance during the recycle delay (RD) of 4 s and the mixing time. The 90° pulse length was adjusted to approximately 10.35 μs. T_1 was set to 4 μs. A total of 4 dummy scans and 256 free induction decays (FIDs) were collected into 120 000 data points, using a spectral width of 10 kHz, giving an acquisition time (ACQ) of 6.13 s. All NMR experiments were conducted at 298K on a Bruker (Karlsruhe, Germany) Avance III 500-MHz spectrometer equipped with an ultra-low-temperature probe.

Spectral data processing and multivariate statistical analysis

To improve the signal-to-noise ratio, all 1D FIDs were multiplied by an exponential weighting factor of a 0.3 Hz line-

broadening factor before Fourier transformation. Then, all the 1D NMR spectra were referenced to the methyl group of lactate at δ 1.33, carefully manually phased, baseline corrected and aligned by MestReNova software (Version 8.0, Mestrelab Research SL). Selected peaks without overlap for each metabolite in the 1D NMR were integrated. The resulting unambiguous 39 metabolites in liver extracts and 31 metabolites in heart extracts were normalized to the sum of the spectral intensity (excluding the regions of the residual water, methanol and ethanol resonances) to compensate for differences in sample concentration. Subsequently, the normalized integral values were invariably scaled for PCA, PLS-DA, and OPLS-DA by SIMCA-P+12.0 software package (Umetrics, Umeå, Sweden). The PCA and PLS-DA score plots were visualized with the first principal component (t[1]) and the second principal component (t[2]). The OPLS-DA was calculated with the first predictive (t[1]) and one orthogonal component (to[1]). The parameters R2X(cum), R2Y(cum) and Q2(cum) were calculated by following the cross-validation procedure to test the goodness of fit and model validity. R2X(cum) and R2Y(cum) are the fraction of the sum of the squares of the entire X's and Y's explained by the model, respectively. Q2(cum) represents the cross-validated explained variation. The reliability of models increases as R2Y(cum) and Q2(cum) approach 1[32]. Due to the small number of samples (CS:OP:SO=6:7:7), five-round cross validation and permutation tests (500 cycles) were carried out to measure the robustness of the models[33].

The correlation coefficients of the variables relative to the first predictive component in the OPLS-DA model were extracted from S-plot. Cutoff values with a significance level of 0.05 were used to identify those variables that were responsible for the discrimination of the groups[34]. Variable importance in the projection (VIP) values were also employed to identify the differentiating biomolecules with a VIP value greater than 1, which contributed significantly to model clustering. Therefore, we chose those variables meeting twofold criteria (*ie*, |r|>=the cutoff value of *P*=0.05, and VIP>=1) as the most significant and reliable variables that were responsible for the separation of the clusters.

Quantitative comparison of metabolites in ^{1}H NMR spectra of liver and heart aqueous extract samples

The average changes of metabolites between two groups were calculated[35]. Box charts were used to depict the variation in the integrals of the most significant metabolites in the CS, OP, and SO groups, which are shown in Figure 4. Significant differences (Table 1) among the mean values (Table S1) were evaluated by one-way analysis of variance (ANOVA) with a Bonferroni correction. The threshold for statistical significance was set to *P*<=0.05. All the statistical analyses were performed using SPSS (Statistical Package for the Social Sciences) 17.0 software (SPSS, Chicago, IL, USA).

The ranks of statistical significance were then divided into three degrees: statistical significance with VIP>=1, |r|>=the cutoff value and *P*<=0.05 was defined as "remarkable"; significance with VIP>=1, |r|>=the cutoff value and *P*>0.05 was defined as "moderate"; and significance with VIP>=1 and |r|<the cutoff value was defined as "weak.

Results

^{1}H NMR spectra of tissue aqueous extract samples

Representative (of three) one-dimensional ^{1}H NMR spectra of liver tissue aqueous extracts obtained from the CS, OP, and SO groups are shown in Figure 1, while 1D ^{1}H NMR spectra of heart aqueous extract samples are illustrated in Figure S2. The metabolite resonances were annotated based on chemical shifts, proton-proton coupling constants, results from 2D NMR spectra and published data[36–38]. The assignments (both chemical shift and multiplicity) for the identified metabolites are summarized in Table S2. The NMR spectra of the aqueous tissue extracts were dominated by the signals from amino acids (leucine, isoleucine, valine, alanine, lysine, glutamine, glutamate, glycine, aspartate, phenylalanine and tyrosine), carboxylic acids (α-hydroisobutyrate, acetate, succinate, malate, fumarate, D-3-hydrobutyrate, formate, lactate), membrane components (choline, sn-glycero-3-phosphocholine, *O*-phosphocholine), oxidative stress metabolites (glutathione and taurine), nitrogen-containing heterocycles [nicotinamide adenine dinucleotide (NAD), NADP+, nicotinurate, adenosine triphosphate (ATP)] and so on. The characterization of a metabolic profile based on such complicated spectra could be greatly facilitated by multivariate statistical analyses, such as PCA, PLS-DA, and OPLS-DA. Thus, the integral data for the metabolites were imported into the SIMCA-P+12.0 software package for statistical analysis. One-way analysis of variance using a Bonferroni *post hoc* test was also performed to determine whether group-to-group differences in the mean values of the metabolites were significant.

Statistical analysis of liver aqueous extract samples

The PCA score plots, which were obtained from the multivariate statistical analysis of the unambiguously identified 39 variables from the liver aqueous extracts of the three groups, revealed a group clustering for the metabolic profiles of the OP group versus the SO group samples (Figure S3A). Consistently, a distinct separation between the OP group and the SO group was also present in the PLS-DA score plot along the PC1 axis, and, in comparison with the OP group, the CS group cluster moved closer to that of the SO group, indicating that *C sinensis* administration ameliorated the metabolic disorders in the liver tissue of CKD rats (Figure 2A).

The results mentioned above were supported by the following OPLS-DA analysis. The application of OPLS-DA, which used the first predictive component and one orthogonal component to optimize intergroup variation, resulted in clear biochemical distinctions between the CS and OP groups [R2X(cum)=40%, R2Y(cum)=90%, Q2(cum)=52%] (Figure 3A) and between the OP and SO groups [R2X(cum)=47%, R2Y(cum)=97%, Q2(cum)=85%] (Figure 3C). A cluster of 500 permutated models from the first component was visualized using validation plots (Figures 3B, 3D). In the permutation test plots, all of the permutated Q2 values to the left were

Table 1. The average changes of main metabolites in OPLS-DA models.

Meta bolites	δ ^{1}H (ppm)	Aqueous liver extract		Aqueous heart extract	
		% Average changes in CS relatively to OP (|r|, VIP, *P*)	% Average changes in OP relatively to SO (|r|, VIP, *P*)	% Average changes in CS relatively to OP (|r|, VIP, *P*)	% Average changes in OP relatively to SO (|r|, VIP, *P*)
Leu	0.96	−20.8 (0.83, 1.64, 0.010)	+45.6 (0.85, 1.48, 0.000)	/	/
Ile	1.02	−13.9 (0.63, 1.04, 0.086)	+38.3 (0.71, 1.31, 0.001)	/	/
Val	1.05	−27.6 (0.91, 1.89, 0.004)	+63.8 (0.79, 1.47, 0.000)	/	/
Ala	1.49	/	/	/	+17.5 (0.75, 1.21, 0.023)
Lys	1.72	−13.8 (0.63, 1.14, 0.043)	+57.0 (0.83, 1.54, 0.000)	−28.4 (0.55,1.34,0.020)	/
NAG	2.08	+20.7 (0.57, 1.39,0.109)	−34.5 (0.74, 1.41, 0.000)	/	/
Glu	2.36	/ (0.08,0.51,1.000)	-41.1 (0.64, 1.34, 0.004)	/	/
Suc	2.40	/	/	/	+50.0 (0.76, 1.45, 0.025)
Gln	2.45	/ (0.10, 0.23,1.000)	−29.0 (0.74, 1.41, 0.003)	/	/
GSH	2.54	+13.8 (0.52,1.13, 0.215)	−30.7 (0.77, 1.45, 0.000)	/	/
Sar	2.74	−23.6 (0.54,1.02, 0.180)	+97.4 (0.76, 1.49, 0.000)	/	/
DMG	2.93	/ (0.26, 0.49,1.000)	+41.6 (0.67, 1.28, 0.014)	/	/
Cr	3.95	/ (0.41, 0.99, 1.000)	-64.8 (0.68, 1.35, 0.001)	/	−8.7 (0.78, 2.21, 0.024)
Cho	3.21	−41.2 (0.74, 1.32, 0.023)	+185.4 (0.83, 1.57, 0.000)	/	/
Pcho	3.22	−22.8 (0.61,1.34, 0.044)	/	/	/
Car	3.20	+41.5 (0.76, 1.64, 0.020)	−35.1 (0.66, 1.27, 0.000)	/	/
Tau	3.43	+40.5 (0.59, 1.19, 0.026)	−30.4 (0.66, 1.11, 0.01)	+15.9 (0.58, 1.82, 0.038)	−5.7(0.78, 2.47, 0.057)
Gly	3.57	+22.4 (0.64, 1.54, 0.024)	/ (0.02, 0.02, 1.000)	/	/
UDPG	5.92	/ (0.48, 0.95, 0.288)	−35.4 (0.70, 1.33, 0.000)	/	/
Tyr	6.89	−52.5 (0.74, 1.49, 0.014)	+105.9 (0.75, 1.40, 0.007)		
ATP	8.58	+60.6 (0.45, 0.83, 0.317)	−31.7 (0.45, 1.00, 0.390)	/	/
NAD	9.36	+23.5 (0.57, 1.23, 0.023)	−21.9 (0.70, 1.26, 0.004)	/	/

Leu, leucine; Ile, isoleucine; Val, valine; Ala, alanine; Lys, lysine; NAG, *N*-acetylglutamine; Glu, glutamate; Suc, succinate; Gln, glutamine; GSH, glutathione; Sar, sarcosine; DMG, *N*,*N*-dimethylglycine; Cr, creatine; Cho, choline; Pcho, *O*-phosphocholine; Car, carnitine; Tau, taurine; Gly, glycine; UDPG, UDP-galactose; Tyr, tyrosine; ATP, adenosine triphosphate; NAD, nicotinamide adenine dinucleotide.

"+" means an increase. "−" means a decrease. "/" means no significant change (|r|<the cutoff value, VIP<1, and *P*>0.05).

[a] The absolute values of correlation number extracted from the correlation plots of OPLS-DA models. The cutoff values are 0.55 in the correlation-loading plot of CS *vs* OP and 0.53 in the correlation-loading plot of OP *vs* SO.

[b] The *P* values were obtained from one way ANOVA.

lower than the original point to the right[39, 40], which indicated that the original models were valid.

Moreover, according to coefficient numbers (|r|), VIP and *P* values, the major discriminatory metabolites for each group were determined in the pair-wise comparison. Compared with the SO group, the levels of leucine, isoleucine, valine, lysine, sarcosine, *N*,*N*-dimethylglycine, choline and tyrosine were upregulated in the OP group. The levels of certain metabolites including N-acetylglutamine, glutamate, glutamine, glutathione, creatine, carnitine, taurine, UDP-galactose, ATP and NAD declined (Table 1). After *C sinensis* administration, there was a reversal of the changes in the levels of several metabolites in the liver of the CKD rats. Compared with the OP rats, the levels of amino acids (leucine, isoleucine, valine, lysine and tyrosine), sarcosine, *O*-phosphocholine and choline in the CS group declined, and these changes were accompanied by increases in the levels of *N*-acetylglutamine, glutathione, carnitine, taurine, glycine and NAD. Then, referring to the Kyoto Encyclopedia of Genes and Genomes (KEGG) Database[41] and the Human Metabolome Database (HMDB)[42], these altered metabolites were connected to different metabolic pathways (Figure 4).

Statistical analysis of ^{1}H NMR data of heart aqueous extract samples

The integrals of 31 metabolites present in the heart tissue extracts were obtained for PCA (Figure S3B) and PLS-DA (Figure 2B) with the first two principal components (t[1], t[2]). The OP rats were metabolically differentiated from the SO rats basically by the first principal component, which was the distinctive feature of the PLS-DA model of the NMR data for the heart aqueous extract samples. Moreover, the three groups displayed separations with a partial overlap in the score plots of the aqueous heart extracts in the PCA scatter plot.

To assess the variations between groups, permutation tests were applied, and the ensuing results (Figure S4B) strongly indicated that the OPLS-DA model (Figure S4A) of the CS *vs* OP group were overfitting, as demonstrated by the fact that the Q2 regression line had a positive intercept and that the Q2 values to the left were higher than the original point to the right. Additionally, there were only a few altered metabolites that contributed to the separation, and these were identified by

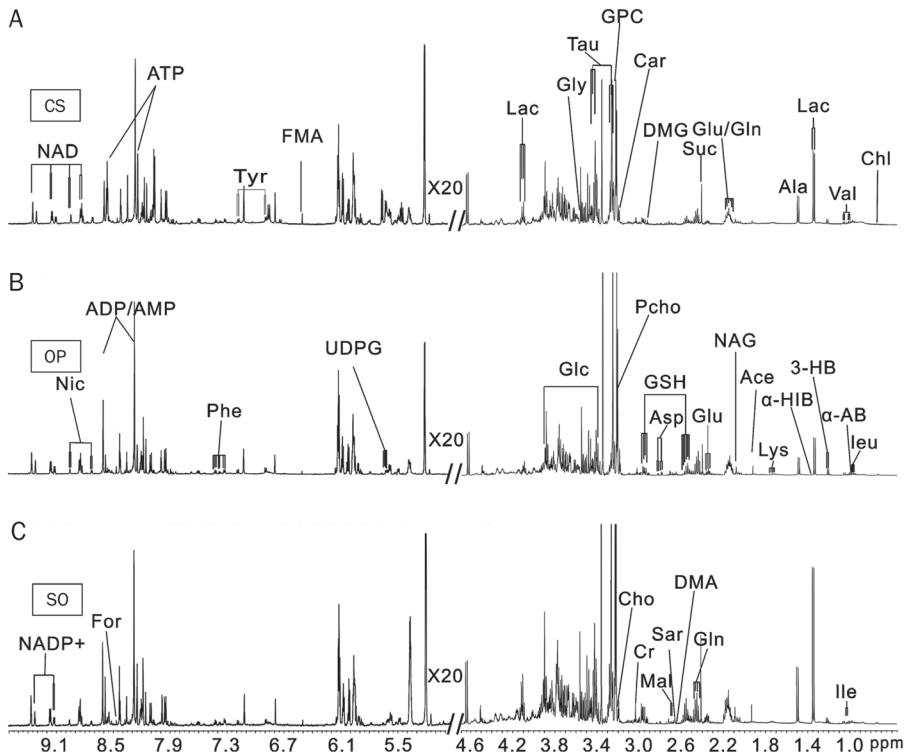

Figure 1. Representative 500-MHz ^{1}H NMR NOESY spectra (δ 0.6–4.7, 5.0–9.6) of aqueous extracts from liver tissues of rats in groups CS (A), OP (B) and SO (C). The abbreviations of the metabolites are shown in Table S1.

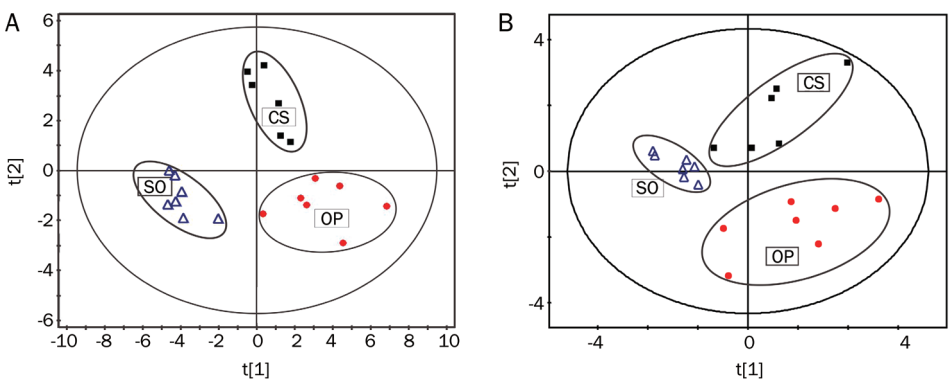

Figure 2. PLS-DA score plots of ^{1}H NMR analysis of aqueous liver extracts (A) and aqueous heart extracts (B). Model parameters are as follows: (A) R2X(cum)=0.37, R2Y(cum)=0.82, Q2(cum)=0.57; (B) R2X(cum)=0.52, R2Y(cum)=0.60, Q2(cum)=0.22.

the coefficient number, the VIP value, and the *P* value. Compared with the SO rats, the prominent changes in the OP rats were increasing levels of alanine and succinate and decreasing levels of creatine and taurine. Moreover, the change in taurine levels was reversed by the administration of *C sinensis* (Table 1).

Discussion

The results of the metabolomic analyses indicated that in the experimental time scale (8 weeks), the metabolic disorders in the liver were more significant than those in the heart, which suggested that 8 weeks after 5/6Nx operation, liver dysfunction had already progressed, while heart injury was in the early stages of initiation. It appeared that CKD-related extrarenal organ dysfunctions occurred sequentially rather than simultaneously.

In this study, we hoped to unravel the mechanism of by which *C sinensis* modulates metabolism in the extrarenal organs of CKD rats using ^{1}H NMR-based metabolomic analysis. Both multivariate and univariate statistical analyses of the data and subsequent pathway mapping of the perturbed metabolites indicated that the metabolic differences were

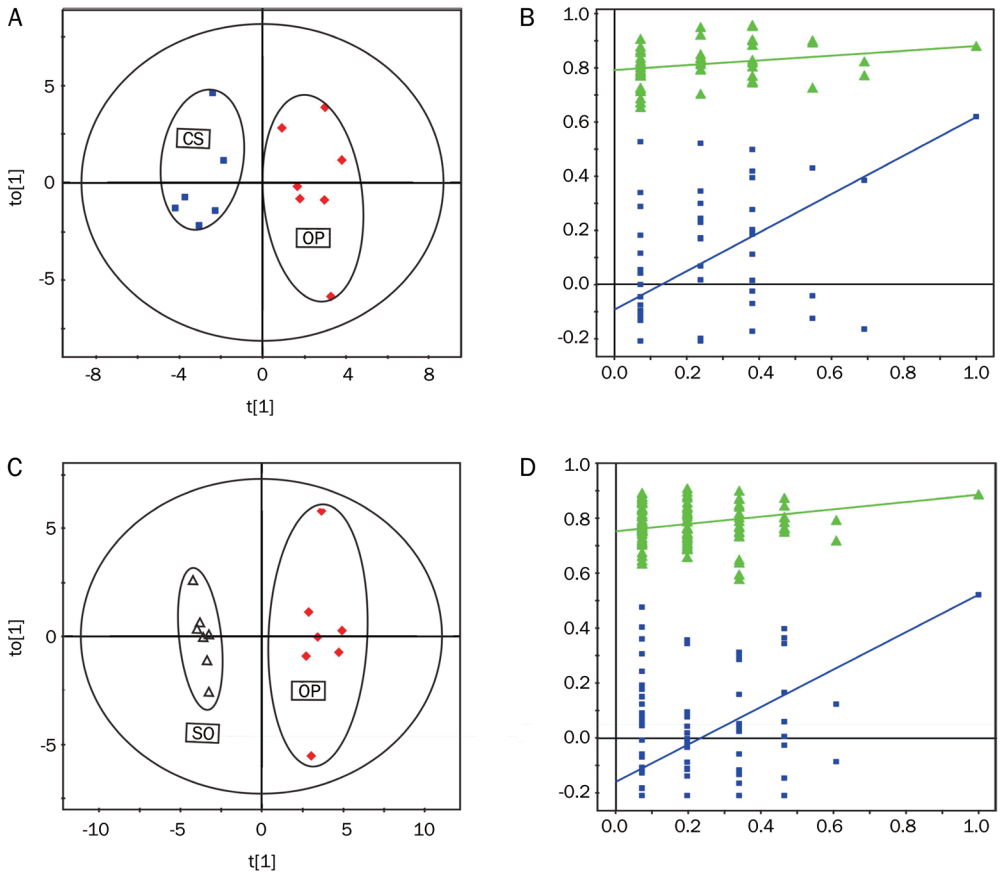

Figure 3. The score plots (left) and the permutation tests (right) derived from OPLS-DA models of (A, C) CS *vs* OP with the 5-round cross validation, (B, D) OP *vs* SO with the 5-round cross validation of ^{1}H NMR spectra of aqueous liver extracts. Variables of score plots are autoscaling all variables to unit variance.

mainly from oxidative stress-related metabolites, energy metabolism intermediates, amino acid and protein metabolites and choline metabolites. The disturbed metabolites in the liver and heart tissues and the ones substantially reversely regulated by the administration of *C sinensis* could be taken as a pool of potential candidates for the development of clinical biomarkers for the diagnosis of CKD and for the discovery of therapeutic targets for treatment of CKD-related extrarenal organ damage.

Antioxidative activity

Glutathione (GSH) is a predominant antioxidant that protects against reactive species and oxidative stress[43]. Previously reported work demonstrated that hepatic glutathione was significantly decreased in alcoholic liver disease[44], hepatic veno-occlusive disease[45], chronic hepatitis C[46], Wilson's disease[47] and other liver-related diseases. The significant depletion of hepatic glutathione in the OP rats was a marker of the disruption of cellular redox status related to CKD-induced liver injury. However, increased glutathione turnover was observed in CS rats, which implied that *C sinensis* mitigated CKD-related liver injury via its antioxidative activity[48].

Taurine, a free amino acid, is known to counteract oxidative stress in tissues (liver, kidney and retina)[49, 50]. As reported by Rashid *et al*, taurine may ameliorate oxidative stress in the complications of diabetic-induced liver injury[51]. Increased levels of taurine in CKD patients were reported as a cure for ameliorating oxidative stress[52]. The significant upregulation of the level of taurine was detected in the livers and hearts of CS group rats, which suggested that taurine potentially contributed to the rescue effects of *C sinensis* on CKD-induced hepatic damage and heart dysfunction by mitigating oxidative stress.

Overall, glutathione and taurine could serve as biomarkers of oxidative stress in OP group rats. *C sinensis* showed protective effects against CKD-induced liver damage by modulating the levels of these metabolites related to oxidative stress. In fact, Yu *et al*[53] reported that some components isolated from *C sinensis*, such as flavonoids and polyphenolics, showed high anti-oxidative effects, especially in the scavenging of hydroxyl radicals.

Energy metabolism

In the hepatic cell, glutamine can be converted to glutamate, which is a major cell energy substrate via anapleurotic input into the tricarboxylic acid (TCA) cycle[54]. Because the levels of

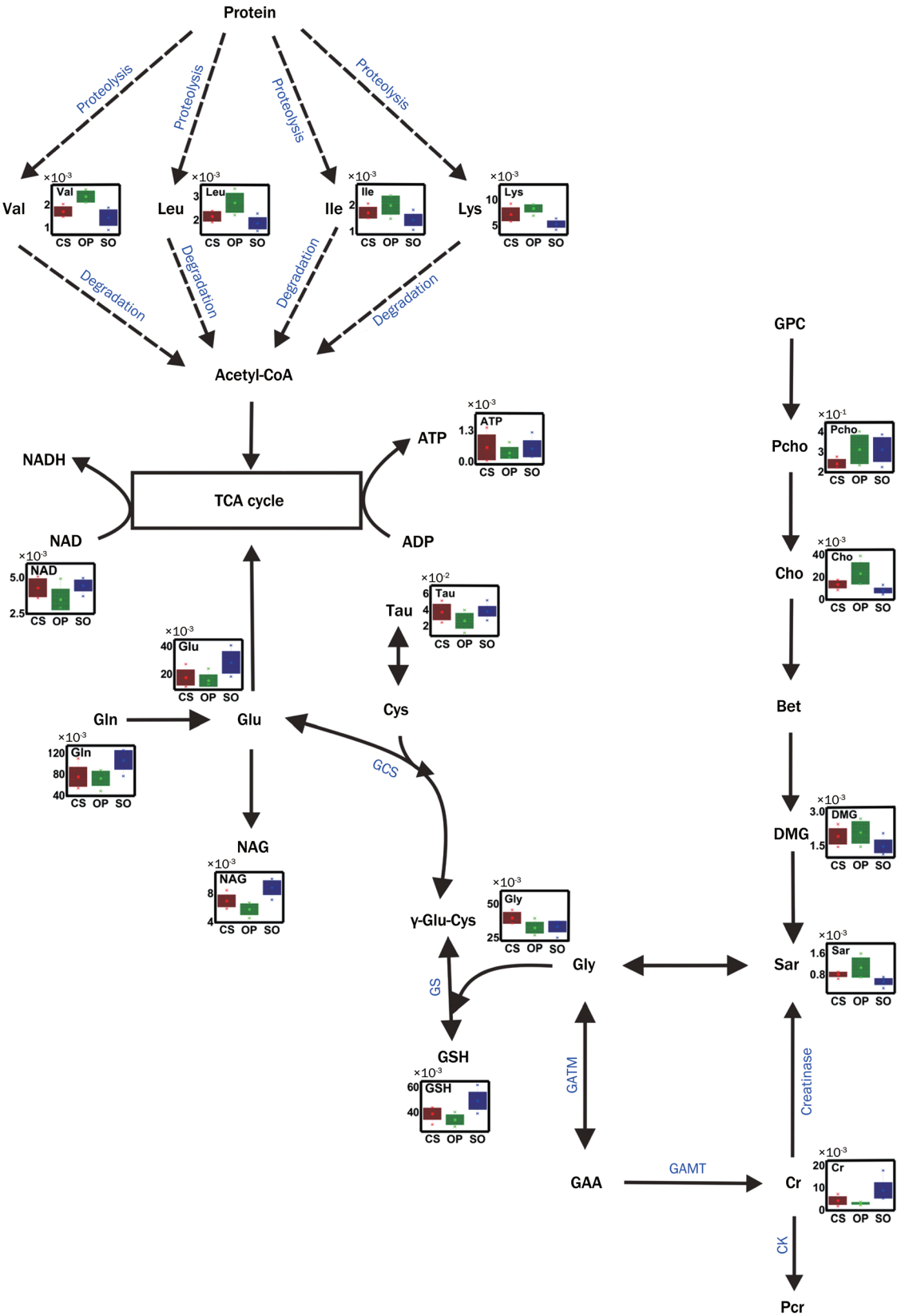

Figure 4. Potential metabolic pathways disturbed in the OP group and altered in the CS group. Abbreviations: GCS, γ-glutamylcysteine synthetase (EC: 6.3.2.2); GS, glutathione synthetase (EC: 6.3.2.3); GATM, glycine amidinotransferase (EC: 2.1.4.1); GAMT, guanidinoacetate *N*-methyltransferase (EC: 2.1.2.2); CK, Creatine kinase (EC: 2.7.3.2); Cr, Creatinase (EC: 3.5.3.3); Pcr, Phosphocreatine. The abbreviations of other metabolites are denoted in Table S1.

the measured TCA cycle intermediates (ie, malate and fumarate) did not significantly vary between the OP group and SO group, and because decreased levels of glutamine and glutamate were observed in the livers of OP rats, we propose that the shifts of glutamine and glutamate into the TCA cycle in the OP rats may help maintain the homeostasis of the TCA cycle. Moreover, glutaminolysis also contributes to the production of mitochondrial NAD, which is used to support ATP production by oxidative phosphorylation. However, NAD, as a key component of energy metabolism[55], was significantly downregulated in the liver tissues from OP rats, and this change may be closely related to the decreased levels of ATP in the liver. The augmented levels of NAD found in the CS group could directly be attributed to energy metabolism recovery after *C sinensis* treatment.

L-carnitine is a metabolite that is critical for lipid metabolism, as it facilitates the transport of fatty acids into the mitochondrion, where β-oxidation occurs[56]. Hepatic damage causes a decrease in *L*-carnitine levels[57], which was observed in the livers from rats in the OP group. The decrease in carnitine levels may prevent β-oxidation of lipids in the OP group, which in turn contributed to the observed energy insufficiency and liver damage. However, after administration of *C sinensis*, the levels of *L*-carnitine were upregulated towards normal levels, which may account for the hepato-protective effects of *C sinensis*. In summary, *C sinensis* increased energy metabolism to support the recovery of function in the damaged liver.

Amino acid and protein metabolism

Compared with the SO group, the significantly increased levels of amino acids including tyrosine, lysine, isoleucine, leucine, valine (in the livers) and alanine (in the hearts) were observed in tissues from OP rats (Table 1). Because the wide variety of free amino acids are important precursors and can be exhausted as substrates for energy supplementation, excessive consumption of amino acids would lead to an upregulation of proteolysis in the damaged liver (Figure 4). In agreement with this finding, creatine, as a nitrogenous compound, also showed a significant reduction in the liver of OP rats, which suggested that protein metabolism was dramatically affected. After administration of *C sinensis*, the levels of the five perturbed amino acids were downregulated towards normal, which was a distinct metabolic feature of the CS group versus the OP group indicating improved amino acid and protein metabolism in CS rats.

Choline metabolism

The elevated levels of choline in the OP rats may have resulted from disturbances of the metabolism of membrane phospholipids. Choline can be degraded to *N,N*-dimethylglycine via sarcosine. In the present study, the levels of *N,N*-dimethylglycine, sarcosine and choline were significantly increased in the livers from OP rats. However, compared with the OP group, the CS group showed decreased levels of *O*-phosphocholine, choline and sarcosine, indicating that disturbed choline metabolism was partially recovered by treatment with *C sinensis*.

Conclusion

In the present work, ^{1}H NMR-based metabolomic analysis was applied to an investigation of the metabolic effects of *C.sinensis* in CKD-induced liver and heart injuries. The changes in metabolic patterns, fluctuations in levels of endogenous metabolites and altered pathways in *C sinensis*-dosed 5/6Nx rats and CKD-modeled rats were identified using a combination of PCA, PLS-DA, and OPLS-DA methods. Oxidative stress, energy metabolism, amino acid and protein metabolism and choline metabolism may be considered as links between CKD and extrarenal organ dysfunction. By modulating these pathways, *C sinensis* exerted its protective effects on extrarenal organs. Moreover, our work also demonstrated that the established ^{1}H NMR-based metabolomics approach can provide a systematic and holistic view for a greater understanding of disease and drug treatment, and the methodology can also be applied to extensively investigate the salutary mechanisms of action of traditional Chinese medicines.

Acknowledgements

We thank Jerry LANGE for proofreading. This work was financially supported by the National Natural Science Foundation of China (Grant No 30900662), the Shanghai Foundation for Development of Science and Technology (Grant No 08411965600) and the "100 Talents Program" of the Chinese Academy of Sciences.

Author contribution

Xia LIU, Fang ZHONG, Xu-long TANG, Wei-ming WANG, Nan CHEN, and Nai-xia ZHANG conceived and designed the experiments; Xia LIU, Fang ZHONG, Xu-long TANG, Fu-lin LIAN, Qiao ZHOU, Shan-mai GUO, Peng SUN, Xu HAO, Ying LU performed the experiments; Xia LIU, Nai-xia ZHANG analyzed the data; Jia-fu LIU proofread the manuscript; Xia LIU and Nai-xia ZHANG wrote the manuscript.

Supplementary information

Supplementary information is available at Acta Pharmacologica Sinica's website.

References

1 Kelly KJ. Acute renal failure: much more than a kidney disease. Semin Nephrol 2006; 26: 105–13.
2 Levin A, Djurdjev O, Barrett B, Burgess E, Carlisle E, Ethier J, *et al*. Cardiovascular disease in patients with chronic kidney disease: Getting to the heart of the matter. Am J Kidney Dis 2001; 38: 1398–407.
3 Hruska KA, Korkor A, Martin K, Slatopolsky E. Peripheral metabolism of intact parathyroid hormone. Role of liver and kidney and the effect of chronic renal failure. J Clin Invest 1981; 67: 885–92.
4 Nair KS. Amino acid and protein metabolism in chronic renal failure. J Renal Nutr 2005; 15: 28–33.
5 Zhao YY, Feng YL, Bai X, Tan XJ, Lin RC, Mei Q. Ultra performance liquid chromatography-based metabonomic study of therapeutic effect of the surface layer of *Poria cocos* on adenine-induced chronic kidney disease provides new insight into anti-fibrosis mechanism. PLoS One 2013; 8: e59617.
6 Zhao YY, Lei P, Chen DQ, Feng YL, Bai X. Renal metabolic profiling of

early renal injury and renoprotective effects of *Poria cocos* epidermis using UPLC Q-TOF/HSMS/MSE. J Pharm Biomed Anal 2013; 81–82: 202–9.

7 Zhao YY, Shen XF, Cheng XL, Wei F, Bai X, Lin RC. Urinary metabonomics study on the protective effects of ergosta-4,6,8(14),22-tetraen-3-one on chronic renal failure in rats using UPLC Q-TOF/MS and a novel MSE data collection technique. Process Biochem 2012; 47: 1980–87.

8 Zhao YY, Feng YL, Du X, Xi ZH, Cheng XL, Wei F. Diuretic activity of the ethanol and aqueous extracts of the surface layer of *Poria cocos* in rat. J Ethnopharmacol 2012; 144: 775–8.

9 Zhong F, Liu X, Zhou Q, Hao X, Lu Y, Guo S, *et al.* ^{1}H NMR spectroscopy analysis of metabolites in the kidneys provides new insight into pathophysiological mechanisms: applications for treatment with *Cordyceps sinensis*. Nephrol Dial Transplant 2012; 27: 556–65.

10 Li FH, Liu P, Xiong WG, Xu GF. Effects of *Cordyceps sinensis* on dimethylnitrosamine-induced liver fibrosis in rats. Zhong Xi Yi Jie He Xue Bao 2006; 4: 514–7.

11 Yan XF, Zhang ZM, Yao HY, Guan Y, Zhu JP, Zhang LH, *et al.* Cardiovascular protection and antioxidant activity of the extracts from the mycelia of *Cordyceps sinensis* act partially via adenosine receptors. Phytother Res 2013; 27: 1597–604.

12 Zhang Z, Xia SS. *Cordyceps sinensis*-I as an immunosuppressant in heterotopic heart allograft model in rats. J Tongji Med Univ 1990; 10: 100–3.

13 Huang Q, Tan Y, Yin P, Ye G, Gao P, Lu X, *et al.* Metabolic characterization of hepatocellular carcinoma using nontargeted tissue metabolomics. Cancer Res 2013; 73: 4992–5002.

14 Maekawa K, Hirayama A, Iwata Y, Tajima Y, Nishimaki-Mogami T, Sugawara S, *et al.* Global metabolomic analysis of heart tissue in a hamster model for dilated cardiomyopathy. J Mol Cell Cardiol 2013; 59: 76–85.

15 Zhao YY. Metabolomics in chronic kidney disease. Clin Chim Acta 2013; 422: 59–69.

16 Zhao YY, Cheng XL, Wei F, Bai X, Tan XJ, Lin RC, *et al.* Intrarenal metabolomic investigation of chronic kidney disease and its TGF-beta1 mechanism in induced-adenine rats using UPLC Q-TOF/HSMS/MSE. J Proteome Res 2013; 12: 692–703.

17 Mutsaers HA, Engelke UF, Wilmer MJ, Wetzels JF, Wevers RA, van den Heuvel LP, *et al.* Optimized metabolomic approach to identify uremic solutes in plasma of stage 3–4 chronic kidney disease patients. PLoS One 2013; 8: e71199.

18 Qi S, Ouyang X, Wang L, Peng W, Wen J, Dai Y. A pilot metabolic profiling study in serum of patients with chronic kidney disease based on (1) H-NMR-spectroscopy. Clin Transl Sci 2012; 5: 379–85.

19 Zhao YY, Liu J, Cheng XL, Bai X, Lin RC. Urinary metabonomics study on biochemical changes in an experimental model of chronic renal failure by adenine based on UPLC Q-TOF/MS. Clin Chim Acta 2012; 413: 642–9.

20 Creek DJ, Barrett MP. Determination of antiprotozoal drug mechanisms by metabolomics approaches. Parasitology 2014; 141: 83–92.

21 Beyoglu D, Idle JR. Metabolomics and its potential in drug development. Biochem Pharmacol 2013; 85: 12–20.

22 Gu Y, Zhang Y, Shi X, Li X, Hong J, Chen J, *et al.* Effect of traditional Chinese medicine berberine on type 2 diabetes based on comprehensive metabonomics. Talanta 2010; 81: 766–72.

23 Zhao X, Zhang Y, Meng X, Yin P, Deng C, Chen J, *et al.* Effect of a traditional Chinese medicine preparation Xindi soft capsule on rat model of acute blood stasis: a urinary metabonomics study based on liquid chromatography-mass spectrometry (Research Support, Non-US Gov't). J chromatogr B 2008; 873: 151–8.

24 Peng SL, Liu XW, Zhang ZR. Investigation of therapeutic mechanism of Weiweifang on experimental gastric ulcer in rats viewing from metabonomics. Zhongguo Zhong Xi Yi Jie He Za Zhi 2010; 30: 1073–7.

25 Lian F, Zhao B, Lu XM. Effect of er'zhi tiangui granule on metabonomics and level of Ca^{2+} in follicle fluid in patients after *in vitro* fertilization and embryo transfer. Zhongguo Zhong Xi Yi Jie He Za Zhi 2010; 30: 22–5.

26 Liang X, Chen X, Liang Q, Zhang H, Hu P, Wang Y, *et al.* Metabonomic study of Chinese medicine Shuanglong Formula as an effective treatment for myocardial infarction in rats. J Proteome Res 2011; 10: 790-9.

27 Manotham K, Eiam-Ong S, Wannakrairot P, Praditpornsilpa K, Chusil S, Tungsanga K. Citrate attenuates tubulointerstitial fibrosis in 5/6 nephrectomized rats by decreasing transforming growth factor-beta1. J Med Assoc Thai 2006; 89 Suppl 2: S168–77.

28 Ghosh SS, Massey HD, Krieg R, Fazelbhoy ZA, Ghosh S, Sica DA, *et al.* Curcumin ameliorates renal failure in 5/6 nephrectomized rats: role of inflammation. Am J Physiol Renal Physiol 2009; 296: F1146–57.

29 Kasiske BL, O'Donnell MP, Garvis WJ, Keane WF. Pharmacologic treatment of hyperlipidemia reduces glomerular injury in rat 5/6 nephrectomy model of chronic renal failure. Circ Res 1988; 62: 367–74.

30 Waldherr R, Gretz N. Natural course of the development of histological lesions after 5/6 nephrectomy. Contrib Nephrol 1988; 60: 64–72.

31 Beckonert O, Keun HC, Ebbels TM, Bundy J, Holmes E, Lindon JC, *et al.* Metabolic profiling, metabolomic and metabonomic procedures for NMR spectroscopy of urine, plasma, serum and tissue extracts. Nat Protoc 2007; 2: 2692–703.

32 Weljie AM, Dowlatabadi R, Miller BJ, Vogel HJ, Jirik FR. An inflammatory arthritis-associated metabolite biomarker pattern revealed by ^{1}H NMR spectroscopy. J Proteome Res 2007; 6: 3456–64.

33 Asiago VM, Alvarado LZ, Shanaiah N, Gowda GA, Owusu-Sarfo K, Ballas RA, *et al.* Early detection of recurrent breast cancer using metabolite profiling. Cancer Res 2010; 70: 8309–18.

34 Cloarec O, Dumas ME, Trygg J, Craig A, Barton RH, Lindon JC, *et al.* Evaluation of the orthogonal projection on latent structure model limitations caused by chemical shift variability and improved visualization of biomarker changes in ^{1}H NMR spectroscopic metabonomic studies. Anal Chem 2005; 77: 517–26.

35 Carrola J, Rocha CM, Barros AS, Gil AM, Goodfellow BJ, Carreira IM, *et al.* Metabolic signatures of lung cancer in biofluids: NMR-based metabonomics of urine. J Proteome Res 2011; 10: 221–30.

36 Ding L, Hao F, Shi Z, Wang Y, Zhang H, Tang H, *et al.* Systems biological responses to chronic perfluorododecanoic acid exposure by integrated metabonomic and transcriptomic studies. J Proteome Res 2009; 8: 2882–91.

37 Fan TWM, Lane AN. Structure-based profiling of metabolites and isotopomers by NMR. Prog Nucl Mag Res Sp 2008; 52: 69–117.

38 Tang HR, Wang YL, Nicholson JK, Lindon JC. Use of relaxation-edited one-dimensional and two dimensional nuclear magnetic resonance spectroscopy to improve detection of small metabolites in blood plasma. Anal Biochem 2004; 325: 260–72.

39 Lindgren F, Hansen B, Karcher W, Sjostrom M, Eriksson L. Model validation by permutation tests: Applications to variable selection. J Chemometr 1996; 10: 521–32.

40 Westerhuis JA, Hoefsloot HCJ, Smit S, Vis DJ, Smilde AK, van Velzen EJJ, *et al*. Assessment of PLSDA cross validation. Metabolomics 2008; 4: 81–9.

41 Okuda S, Yamada T, Hamajima M, Itoh M, Katayama T, Bork P, *et al*. KEGG Atlas mapping for global analysis of metabolic pathways (Research Support, Non-U.S. Gov't). Nucleic Acids Res 2008; 36 (Web

Server issue): W423–6.
42 Wishart DS, Tzur D, Knox C, Eisner R, Guo AC, Young N, *et al*. HMDB: the human metabolome database. Nucleic Acids Res 2007; 35: D521–D26.
43 Mytilineou C, Kramer BC, Yabut JA. Glutathione depletion and oxidative stress. Parkinsonism Relat Disord 2002; 8: 385–7.
44 Shaw S, Rubin KP, Lieber CS. Depressed hepatic glutathione and increased diene conjugates in alcoholic liver disease. Evidence of lipid peroxidation. Dig Dis Sci 1983; 28: 585–9.
45 Wang X, Kanel GC, DeLeve LD. Support of sinusoidal endothelial cell glutathione prevents hepatic veno-occlusive disease in the rat. Hepatology 2000; 31: 428–34.
46 Barbaro G, Di Lorenzo G, Soldini M, Parrotto S, Bellomo G, Belloni G, *et al*. Hepatic glutathione deficiency in chronic hepatitis C: quantitative evaluation in patients who are HIV positive and HIV negative and correlations with plasmatic and lymphocytic concentrations and with the activity of the liver disease. Am J Gastroenterol 1996; 91: 2569–73.
47 Summer KH, Eisenburg J. Low content of hepatic reduced glutathione in patients with Wilson's disease. Biochem Med 1985; 34: 107–11.
48 Lanza IR, Zhang SC, Ward LE, Karakelides H, Raftery D, Nair KS. Quantitative metabolomics by H-1-NMR and LC-MS/MS confirms altered metabolic pathways in diabetes. PloS One 2010; 5: e10538.
49 Obrosova IG, Fathallah L, Stevens MJ. Taurine counteracts oxidative stress and nerve growth factor deficit in early experimental diabetic neuropathy. Exp Neurol 2001; 172: 211–9.
50 Das J, Ghosh J, Manna P, Sil PC. Acetaminophen induced acute liver failure via oxidative stress and JNK activation: protective role of taurine by the suppression of cytochrome P450 2E1. Free Radical Res 2010; 44: 340–55.
51 Rashid K, Das J, Sil PC. Taurine ameliorate alloxan induced oxidative stress and intrinsic apoptotic pathway in the hepatic tissue of diabetic rats. Food Chem Toxicol 2013; 51: 317–29.
52 Zinellu A, Sotgia S, Loriga G, Deiana L, Satta AE, Carru C. Oxidative stress improvement is associated with increased levels of taurine in CKD patients undergoing lipid-lowering therapy. Amino Acids 2012; 43: 1499–507.
53 Yu HM, Wang BS, Huang SC, Duh PD. Comparison of protective effects between cultured *Cordyceps militaris* and natural *Cordyceps sinensis* against oxidative damage. J Agr Food Chem 2006; 54: 3132–8.
54 Wisnowski JL, Bluml S, Paquette L, Zelinski E, Nelson MD Jr, Painter MJ, *et al*. Altered glutamatergic metabolism associated with punctate white matter lesions in preterm infants. PLoS One 2013; 8: e56880.
55 Poole RK, Haddock BA. Energy-linked reduction of nicotinamide — adenine dinucleotide in membranes derived from normal and various respiratory-deficient mutant strains of *Escherichia coli* K12. Biochem J 1974; 144: 77–85.
56 Serviddio G, Giudetti AM, Bellanti F, Priore P, Rollo T, Tamborra R, *et al*. Oxidation of hepatic carnitine palmitoyl transferase-I (CPT-I) impairs fatty acid beta-oxidation in rats fed a methionine-choline deficient diet. PLoS One 2011; 6: e24084.
57 Lemire J, Mailloux R, Darwich R, Auger C, Appanna VD. The disruption of *L*-carnitine metabolism by aluminum toxicity and oxidative stress promotes dyslipidemia in human astrocytic and hepatic cells. Toxicol Lett 2011; 203: 219–26.